AerospaceEurope Conference2020
BORDEAUX, FRANCE | 25 - 28 FEBRUARY 2020

ON THE DESIGN OF AN ELECTRIC-POWERED MICROFEEDER AIRCRAFT

Alberto Rolando, Francesco Salucci, Lorenzo Trainelli, Carlo E. D. Riboldi, Yasir M. Khan

Department of Aerospace Science and Technology, Politecnico di Milano,
Via G. La Masa 34, 20156 Milano, Italy. Email: alberto.rolando@polimi.it

KEYWORDS: pure-electric, hybrid-electric, microfeeder, aircraft design, innovative propulsion

ABSTRACT:

The present paper focuses on the design of a family of innovative air vehicles conceived to provide a "micro-feeder" service, devised to exploit the existing European network of small local airports as feeders to hubs. Design solutions involving both pure-electric and hybrid-electric powertrains are considered and their relative merits assessed through performance and sensitivity studies. In particular, optimal solutions are contrasted with a retrofit one, showing the advantages provided by a comprehensive, fully coupled approach to electric-powered aircraft preliminary sizing.

1. INTRODUCTION

The "microfeeder" is a novel concept devised in the quest for new, sustainable means fit for a future regional transportation network capable of supporting ambitious societal goals focused on enhanced personal mobility. A prominent example of such goals is represented by the ACARE (Advisory Council for Aviation Research and innovation in Europe) *"4 hours door-to-door"* requirement included in the area "Meeting societal & market needs", which is expressed in the phrase *"90% of travelers within Europe able to complete their journey, door to door, within 4 hours."* [1]

The microfeeder concept is intended to exploit the existing European network of small local airports to provide a widespred transportation service to larger hubs, as an alternative to land-based transportation means, especially for areas that are not served by high-speed trains. The microfeeder service is to be implemented using a new generation, eco-friendly passenger airplane to be specifically designed for a very short-haul mission.

The MAHEPA (www.mahepa.eu) and UNIFIER19 (www.unifier19.eu) projects are peculiar examples of EU-funded H2020 research efforts concerned with such concept. The first provides high-TRL developments in hybrid-electric modular powertrains designed and implemented for 4-seat flying demonstrators and, building on such a strong basis, investigates their scalability to larger airplanes, yearning for regional liners [2]. The second has been recently launched in response to a call for the complete conceptual design of a near-zero emission 19-seater.

The present paper illustrates selected results from the studies related to the design of a microfeeder platform, conceived to be operational in 2025-2030. This specific incarnation of the concept has been carried out through a complete conceptual and preliminary design process, leading to an optimized pure-electric (PE) basic aircraft together with its hybrid-electric (HE) variant. A thorough Europe-based market study analysed passenger traffic flows, routes, airport network, cost, travel time, and competing ground transportation, allowing the determination of the design range and of take-off and landing performance requirements. These, along with other mission profile and payload specifications, provided the basis for a design solution featuring an 8-passenger, twin-propeller, commuter airplane [3].

The following gives a brief account of the design process, in which the PE solution was initially sized and then brought to maturity in a complete preliminary design activity. Based on the PE solution, a HE retrofit was devised employing a serial powertrain based on an internal combustion engine (ICE), allowing a drastic performance enhancement while retaining some of the fundamental low environmental impact advantages. These design solutions are described along with some sensitivity studies showing the effect of some crucial design parameters, in view of a general assessment of their feasibility and capabilities. In addition, the performance of a modified HE version, optimally revised from a preliminary sizing point of view, are contrasted with the previously considered solutions, hinting to the advantages achievable with the use of dedicated design methodologies.

2. PRELIMINARY STUDIES

2.1. Market study

In order to identify the specifications of the sought micro-feeder service and derive appropriate design requirements for the new aircraft, a thorough market study was carried out, targeting the European scenario. First, an analysis on passenger flows was accomplished, aiming to typify the operational niche of the future micro-feeder service. Initially, the

attention was focused on the nine countries which contribute most to passenger traffic: Austria, Belgium, France, Germany, Italy, Netherlands, Spain, Switzerland, and United Kingdom (in alphabetical order).

The main parameters of interest were the airports with higher passenger traffic, the share between domestic and international flights, and the predicted traffic trends. Passenger traffic data was retrieved from [4], together with the information that domestic flights are typically limited below 30% of total flights (much less in smaller countries) with a trend to decrease, mainly due to the increasing availability of high-speed train services. The latter are economically competitive, do not impose restraints on baggage, and are often perceived as offering a more comfortable overall journey.

Nevertheless, [4] also reports that 45% percent of the passenger travels are intra-European. This traffic is concentrated in larger hubs, which process over 50% of the related flights. Indeed, in some cases of relatively smaller countries, such as Belgium and Netherlands, a very limited number of large airports process about 90% of the total number of passengers for that country. A striking example of this phenomenon is shown in Fig. 1 for the case of Netherlands, where the share between the single Amsterdam Schiphol hub and the rest of the country's airports is depicted between the years 2004 and 2015 [5].

Figure 1. Passenger share between airports in the Netherlands (from [5]).

From these considerations, it appears that a market opportunity may exist in providing a feeder service to these large hubs, by exploiting existing small airports that are not currently hosting significant commercial traffic. This new service should be as much as possible low-cost, seamlessly integrated with the served commercial flight network, and environmentally sustainable.

An important socioeconomic effect of a micro-feeding system would be a significant improvement of personal mobility, entailing business and tourist development opportunities. These considerations may apply to other European countries that are currently lesser contributors to passenger traffic and may exploit such a service for boosting internal economy and foreign exchanges alike.

Secondarily, a micro-feeder aircraft may serve as well as a small liner for point-to-point connections, injecting new life to the dropping domestic flight market by offering affordable and comfortable journeys, while substituting older and larger airplanes, which often fly with a lower payload than available (*i.e.* low passenger load factor). In addition to strictly domestic flights, an opportunity may arise in promoting also short-haul international flights between smaller airports. In the European scenario, these are very seldom served by non-stop flights, the typical situation being travelling from the airport of origin to a hub, and then take another flight from there to the airport of destination.

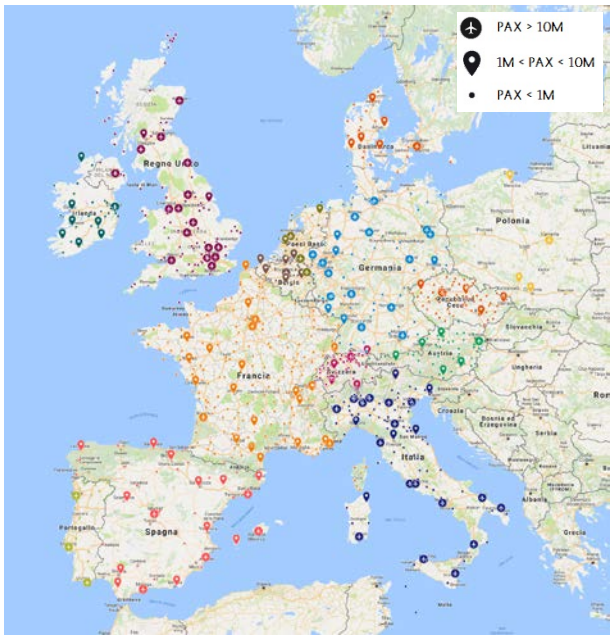

Figure 2. European airport distribution and typology (passenger traffic per year).

Fig. 2 shows the map resulting from a study performed on a larger set of European countries, adding Czech Republic, Denmark, Ireland, Luxembourg, Poland, and Portugal to those previously considered. This allows to broaden the sample with countries that are widely different in population, economy, and air traffic volumes. The map shows all the airports, but not the airfields, such as grass airstrips for light sailplanes, ultra-light (ULM/ML), and light sport aircraft (LSA). It is apparent that Central Europe, including Northern Italy and excluding the former East Germany, is filled with small airports that may harbor a diffuse micro-feeder service, and a potentially widespread point-to-point short haul network as well.

The map has been used to derive a wealth of useful information, such as hub density within each country and distances between each hub and the

rest of the airports. Here, a hub is defined as belonging to the category of larger airports, those serving 10 million passengers/year and above (i.e. the larger marks in Fig. 2). From this analysis, it is seen that Spain and Poland present the lower overall airport density. In Spain, each of the 15 hubs can be reached by at least one of the 22 smaller airports (the smaller marks in Fig. 2) within a range of 104 km. Poland shows a similar situation, with the difference that Spain has a fairly developed high-speed train network, while Poland does not. In contrast, France appears very different in terms of airport density, with its 314 airports (nearly ten times those in Spain, with a territory larger by only 8.5%).

2.2. Performance requirements

The market study allowed the determination of a typical mission range of 250 km, which covers nearly 90% of the short-haul European routes. The proposed vehicle is designed to operate on any airfield, including small, 400 m-long, grassy airstrips, thus enabling its role as a link between major airports and those surrounding areas for which it may provide time and cost advantages over ground transportation.

The typical flight lasts less than 1 hour and involves cruising at 8,000 ft, 200 knots. This, while not necessarily competitive with high-speed trains, may nevertheless be highly convenient where land transportation is still underdeveloped, or hindered by local orography. Attention was given to turnaround time, airport infrastructural needs [6–8], and cost estimates.

Simulations have been carried out for a few test cases in order to verify the time and cost advantages of a microfeeder service fulfilling the above requirements. As an example, the case of a journey from Grosseto (Italy) to either London or Norwich (UK) is reported. Today, the fastest option is to go from Grosseto to Firenze by car, then take a plane to London Stansted, then reach London City or Norwich by train, for a total travel time estimated in 5 hours 15 minutes or 6 hours 15 minutes, respectively. By substituting the first leg with a microfeeder flight, a saving of 100 minutes (31% of the total duration) would be obtained when travelling to London. Substituting also the final leg with another microfeeder flight would result in a saving of nearly three hours (46% of the total duration) when travelling to Norwich. In this case, reaching Norwich from Stansted Airport flying on the microfeeder would be faster than reaching London City by train.

In relation with these observations, a novel methodology to predict the potential demand for a microfeeder service was developed in [9,10]. This takes into account the time advantage of a complete set of potential hub-and-spoke routes in a large geographic area, further justifying the discussed market opportunity.

3. CONCEPTUAL DESIGN

The following introduces the pure-electric (PE) version of the proposed microfeeder aircraft, termed A8E, powered by a battery pack (BP) and sized for the mission requirements emerged from the preliminary studies discussed above [3]. As anticipated, the A8E serves as the baseline for a variant described further on, in which the PE powertrain based on batteries only is substituted with a serial HE one using an ICE-based power generation system (PGS) for range extension.

3.1. Choice of the configuration

The analysis of market opportunities and mission requirements inspired a general configuration with several conventional elements, typical of rugged aircraft in the General Aviation and Commuter categories: “tube and wings” with high, unswept wing, unpressurized cabin, inverted-T tail, twin engines with tractor propellers, tricycle landing gear.

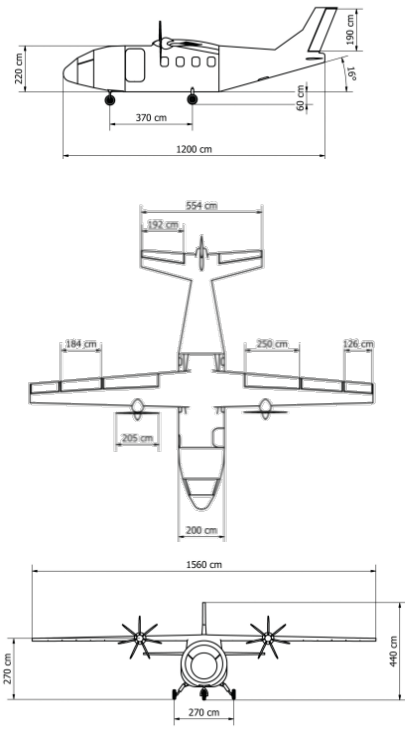

Figure 3. Three views of the proposed microfeeder.

These choices are motivated by the will to limit airframe and system complexity, allow operations on short, possibly grassy airstrips, ease loading/unloading of passenger, cargo, and batteries (particularly meaningful if a BP swapping approach is adopted [6–8]), and provide a familiar global appearance in order to meet customer expectations. Fig. 3 shows the A8E layout, as resulting from the complete preliminary design loop.

3.2. Preliminary sizing

Based on the above considerations, the preliminary sizing of the proposed machine was performed considering applicable performance constraints, including one-engine inoperative conditions, through the application of the HYPERION tool. This is a weight-optimal aircraft sizing procedure dedicated to PE and HE aircraft developed at the Department of Aerospace Science and Technology, Politecnico di Milano, validated and extensively employed in the MAHEPA and UNIFIER19 projects [11].

The output of this tool provides the quantitative aspects of the conceptual design solution: maximum take-off mass (MTOM) and general mass breakdown, total shaft power installed, reference wing surface, as well as a number of other parameters, such as an estimation of the aircraft drag polar. In addition, the procedure yields the detailed time-marching simulation of the design mission, including the time histories of energy and power quantities along the flight, in relation to a specific energy-management strategy [12].

Table 1. Main A8E performance requirements and design specifications.

Stalling CAS @ Landing	60 kn
High-speed cruising CAS	195 kn
High-speed cruising altitude	8,000 ft
Max rate of climb	500 ft/min
Reference climb/descent CAS	160 kn
Take-off length	440 m
Landing length	572 m
Max lift coefficient @ Take-off	2.0
Max lift coefficient @ Landing	2.6
No. of pilots	1
Payload	840 kg
Range	250 km
Loiter altitude	1,000 ft
Loiter duration	10 min
Propeller efficiency	0.85
Electric motor specific power	5,200 W/kg
Battery specific power	1,200 W/kg
Battery specific energy	$1.692 \cdot 10^6$ J/kg

The main input parameters for the A8E are shown in Tab. 1 (CAS stands for calibrated airspeed). These are related not only to mission requirements, but also to CS-23/FAR23 and other applicable specifications. The values for the specific power of the electric motors (EM) reflects current technology, while the combination of specific power and energy of batteries corresponds to Li-S technology in advanced development and considered attainable in a few years [13].

Fig. 4 shows the design point on the sizing matrix plot (SMP), also called performance matching plot, where all point and terminal performance constraints are drawn as functions relating power loading to wing loading [14]. It is seen that the boundaries of the region available for the design are given, by gradually increasing the power loading (i.e. the ratio of maximum take-off weight to installed power), first by the high-speed cruising speed requirement, then by the take-off distance requirement, and finally by the stalling speed requirement which imposes a maximum admissible value to wing loading (i.e. the ratio of maximum take-off weight to the reference wing surface).

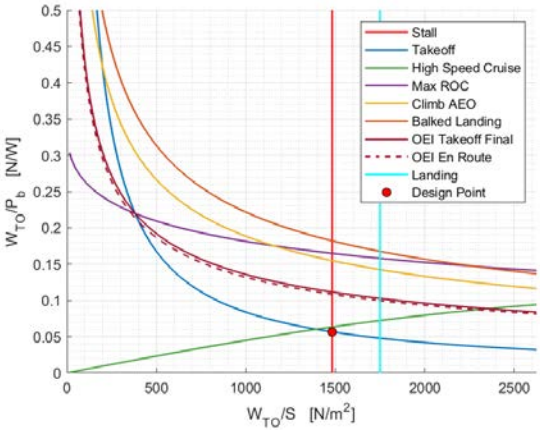

Figure 4. Sizing matrix plot for the proposed microfeeder.

The design point on the SMP has been chosen as the one satisfying the stalling speed constraint characterized by the lowest power loading, with a small safety margin. In other words, once the MTOM is given, the chosen combination corresponding to an aircraft with the smallest wing possible and – among them – to the one with the lower installed shaft power (this being a very common situation).

The outcome of the preliminary sizing loop through HYPERION leads to a MTOM of slightly over 3 tons, an installed EM power of 1.08 kW (which, split in two units, corresponds to product in the class of the Siemens SP260D), and a wing surface of 20.2 m^2. The corresponding mass breakdown shown in Tab 2, first column.

Table 2. Mass breakdown for the A8 variants (kg).

	A8E	**A8H**	**A8HO**
MTOM	3,062	3,062	2,798
NPAM	1,508	1,508	1,308
EMM	104	104	96
PGSM	-	152	139
BPM	614	275	252
FM	-	185	166

The listed quantities are the following: non-propulsive airframe mass (NPAM); mass of the electric motors (EMM); mass of the power generating system (PGSM), for HE aircraft only (absent in the A8E); mass of the battery pack (BPM); and mass of fuel at take-off (FM), for fuel-

burning aircraft only (absent in the A8E). Here, the NPAM is defined as the combination that takes into account of all airframe masses (structure, on-board systems, landing gear, etc.) except those related to the powertrain. As seen, the NPAM amounts to 49.2% of the MTOM, while the airframe mass (AM), here intended as the combination of NPAM and EMM, reaches 52.5% and BPM 20%.

Fig. 5 shows the time evolution of the energy stored on board during the A8E design range mission. The BP state of charge (SOC) is shown, together with the altitude profile. The changes in slope in the BP SOC are clearly related to the changes in flight path angle, with a minor effect seen at the top of climb (due to the close shaft power required values in climb and in high-speed cruise) and a much evident change at the top of descent (where shaft power required for flight decreases more markedly). The altitude profile clearly shows the 10-minute long loiter before mission completion.

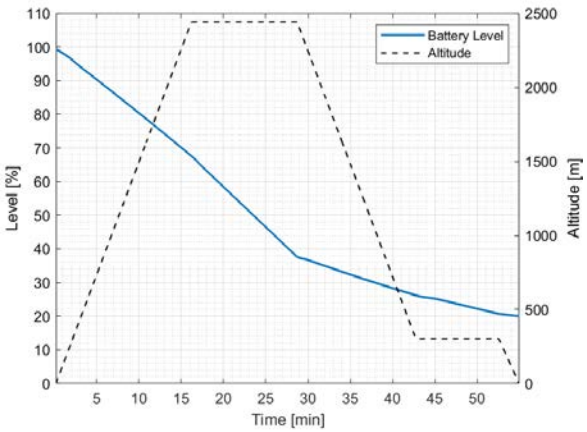

Figure 5. Time histories of battery state of charge (blue) and altitude for the A8E.

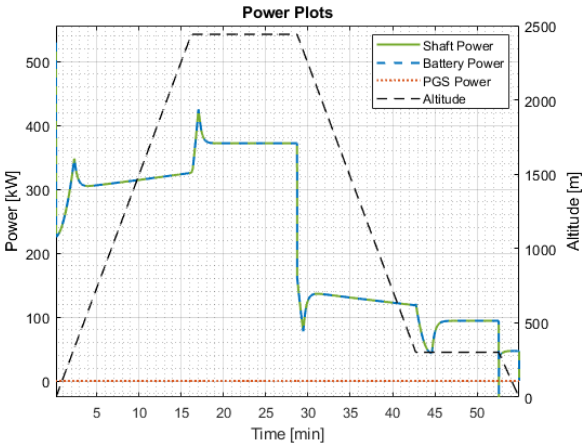

Figure 6. Time histories of shaft power (green), battery power (blue), and altitude for the A8E.

Fig. 6 shows the time evolution of the shaft power required for flight, again constrasted with the altitude profile. The curve named “Battery Power” depicts the time history of the BP power output pre-multiplied by the EM efficiency and, therefore, here coincides with the shaft power. The shaft power clearly follows a trend corresponding to that seen in Fig. 5. The vicinity of the climbing and cruising values compared to the descent values are clearly observed. We remark that the overshoots present at the boundaries of each flight phase are the result of local accelerations and decelerations.

3.3. Sensitivity studies

Sensitivity studies of the design point for the A8E have been carried out by considering variations of a number of design parameters from their reference design values (Tab. 1). Here, the results concerned with battery technology are shown, as they are of capital importance for a pure-electric vehicle.

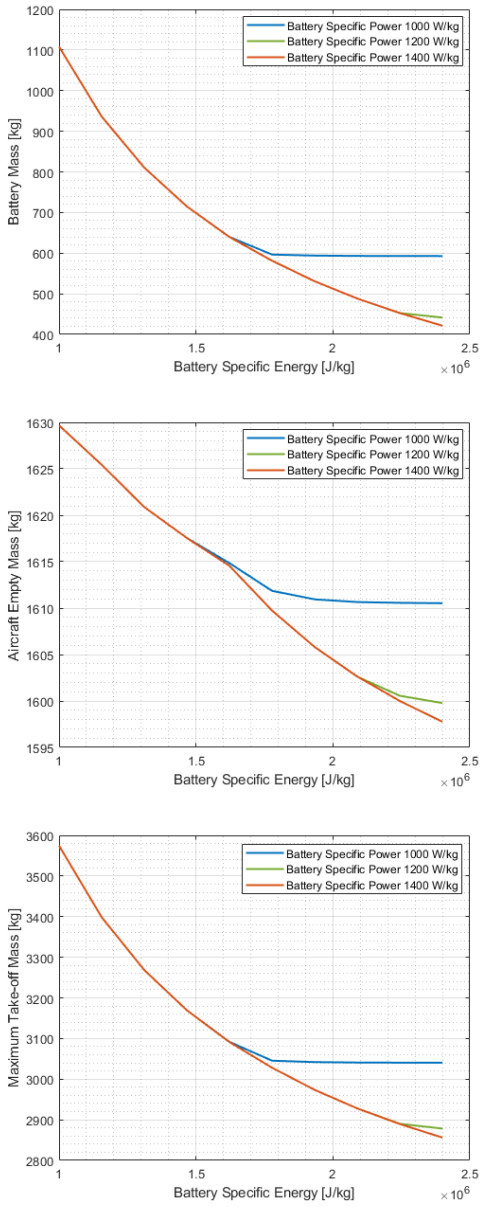

Figure 7. Sensitivity of battery pack mass (top), airframe mass (middle), and maximum take-off mass (bottom) on battery energy and power densities for the A8E.

Fig. 7 shows the trends of BPM, AM, and MTOM

with respect to battery specific energy and specific power. A range in specific energy has been considered in the ±40% neighbourhood of the reference design value, while three values of specific power have been chosen, the reference one and its variations by ±16%.

It is evident that each constant specific-power curve, as specific energy increases, passes by a point characterized by a marked change in slope, after which the curve flattens, showing insensitivity to further rises in specific energy. This behaviour derives from the changes in the BP sizing criterion as the specific power and energies change.

In fact, considering the design specific power value, the A8E design point implies that the BP is sized according to the overall mission energy requirements, entailing that its power output capability exceeds that needed for the mission. Increasing the specific energy at constant specific power, less and less BP mass is necessary, provided that its power output fulfils the mission needs. Thus, a condition is eventually encountered for which the BP power output exactly matches the needs, so that further amelioration of specific energy does not impact on the necessary BP mass anymore. This applies to other values of the specific power, but the change in slope occurs at different specific energy values, which clearly increase as specific power increases.

This behaviour is seen for all mass quantities, although to a lesser extent in magnitude for AM and MTOM when compared to the large effect in BPM. It is remarked with the higher value of specific power, the BPM varies in the range (–31.6%, +79.2%), while AM varies in the range (–0.9%, +1.1%) and the MTOM in the range (–3.3%, +16.9%).

4. ELEMENTS OF PRELIMINARY DESIGN

The choice of the configuration and preliminary sizing of the A8E constitute the basis on which a complete preliminary design loop was carried out, thoroughly considering aerodynamics, powertrain, propellers, structures, on-board systems, and flight mechanics. Here, only a brief account is provided, touching on a few elements of special interest, in order to provide the reader a general view of design choices and outcomes.

For the propulsive system, existing electric motor and battery models were selected and the latter were arranged in 24 packs distributed on the wings and fuselage. A 7-blade optimized propeller was designed in order to meet thrust specifications as well as severe low-noise requirements, fully complying with applicable regulations (Fig. 8).

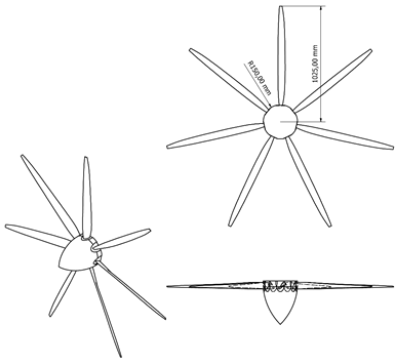

Figure 8. Ad-hoc designed propeller.

Table 3. Propeller far-field noise levels in dB(A).

	Predicted	Limit
Lateral full-power	76	94
Flyover	79	89
Approach	85	98

The promising acoustic performance of this propeller is resumed in Tab. 3, where predicted far-field noise levels are compared with regulation limitations.

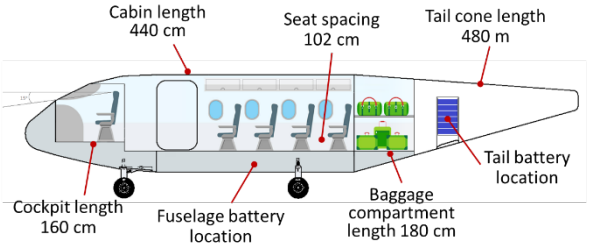

Figure 9. Fuselage configuration of the A8E.

The fuselage layout is depicted in Fig. 9. Mass distribution yields the center of gravity travel seen in Fig. 10, in dependence of the payload amount and distribution.

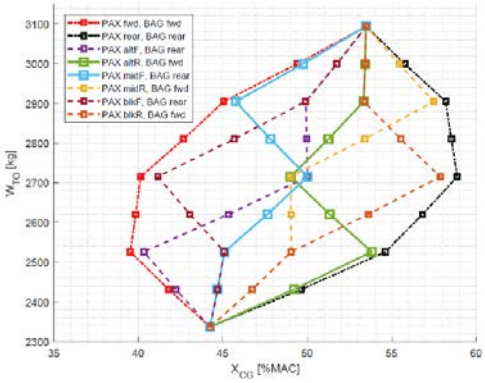

Figure 10. Center of gravity travel for the A8E.

Structural design was carried out by detailed modelling using FEMAP and analysing the full set of manoeuvre and load conditions required by the CS-

23 certification rules using NASTRAN. An example is given in Fig. 11, where the bending moment distribution consequent to the start of a pull-up at manoeuvring airspeed is shown.

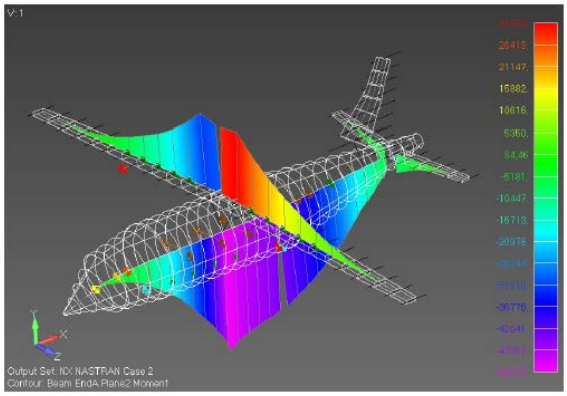

Figure 11. Bending moments loads in a pull-up certification manoeuvre for the A8E.

Critical sections have been identified and used for optimal sizing to manoeuvring loads as well as fatigue, by considering different choices for the material. The outcome features a blend of Al 7075 and Al 2024 for the wing, Al 2024 for the tailplanes, and a blend of Al 2024 and GLARE (glass reinforced aluminium) [15] for the fuselage. Fig. 12 shows the appearance of the resulting complete structural model.

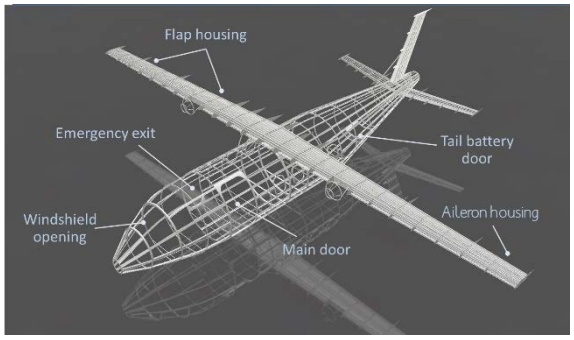

Figure 12. Complete structural model of the A8E.

Further activities included the preliminary design of the landing gear, the flight control system, the environmental control system, and the selection of avionics and cockpit instruments. Basic considerations for subsystem reliability were carried out as well.

Finally, weight and flight performance were verified, confirming full compliance with preliminary sizing estimates. Fig. 13 shows the complete aircraft drag polar for various flap and landing gear configurations.

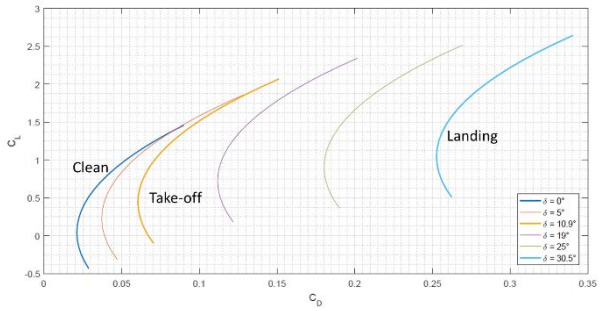

Figure 13. A8E aircraft drag polars according to flap and landing gear configuration.

5. RETROFIT HYBRID-ELECTRIC VERSION

As anticipated, the A8E design solution, fully developed and verified through a complete preliminary design loop, was considered for a retrofit by substituting its PE powertrain with a serial HE propulsion system. This is based on a single ICE for the PGS feeding BP and EMs. Retrofitting here means, above all, that the same MTOM design value applies. Also, the airframe and thrust-generating systems (*i.e.* EMs and propellers) are unchanged with respect to A8E. Payload mass is the same as well. Therefore, in this new aircraft, named A8H, mass breakdown trade-off implies that a significant share of the BPM is substituted with the PGS and fuel tank.

The A8H clearly offers higher range performance due to the more favourable overall specific energy of the HE propulsion system compared with the PE one, at the price of a certain amount of chemical and acoustic emissions. This aspect is mitigated by the ability of a serial HE aircraft to operate in PE mode when close to the ground (i.e. where chemical and acoustic pollution are felt the most). To this end, a transition altitude (TA) is defined, below which PE operations are carried out. This requirement clearly has an effect on the BP sizing.

Running HYPERION under the constraint of constant AM and MTOM values, while setting a TA of 3,000 ft and a stored energy on board at mission completion of 10% of the initial values for both BP and fuel tank, a new sizing point for the A8H is found. This yields the mass breakdown seen in Tab. 2, second column. For this case, given the fact that the BP does not need to sustain the full mission as for the A8E, it was considered convenient to change battery technology and adopt more power-efficient cell types. The specific energy and power values for this type are given in Tab. 4, to be contrasted with the last two rows of Tab 1.

Table 4. Battery performance for the A8 HE variants.

Battery specific power	2193 W/kg
Battery specific energy	$1.260 \cdot 10^6$ J/kg

The A8H provides a maximum range, cruising with full payload at the same altitude and airspeed of the A8E, of 655 km. This will be termed the A8H design range from now on and represents a substantial 162% increase with respect to the A8E.

Fig. 14 shows the time evolution of the energy stored on board during the A8H design range mission. The BP SOC and fuel quantity are shown, together with the PGS throttle level and altitude profile. It can be seen that the PGS is turned on only upon reaching the TA, after a PE take-off and first climb segment. The BP is depleted by over 30% in this initial phase and then restored to 90% SOC (this avoids overstressing the battery cells) thanks to the extra power provided by the PGS with respect to the power required for flight. As apparent, in this case, the recharge is completed quickly, before reaching the top of climb, therefore the PGS is throttled down and then kept to the value corresponding to power required in cruise, Correspondingly, the BP SOC is kept constant. This continues up to the instant in which the energy stored in the BP is sufficient to accomplish the rest of the mission in PE mode. Therefore, as this happens before the top of descent in the present case, the PGS is switched off in the last segment of cruise, to be never called on again. The mission includes a 10 min loiter before final approach and landing, performed in PE mode, as it lies below the TA. The optimality of the sizing process appears also in the fact that the residual BP SOC and fuel exactly match the values imposed. It is remarked that the energy management enforced here corresponds to strategy #3 in [12], which can be demonstrated to be optimal.

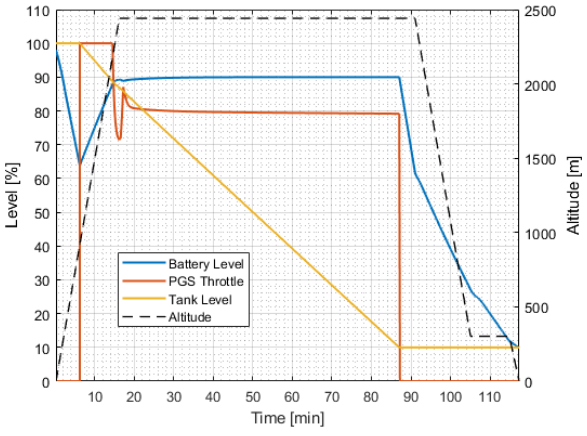

Figure 14. Time histories of battery state of charge (blue), PGS throttle (red), fuel quantity (yellow), and altitude for the A8H.

Fig. 15 shows the time evolution of the power delivered by the two sources on board, contrasted with the shaft power required for flight and the altitude profile. BP and PGS activities clearly follow trends corresponding to those seen in Fig. 14. Note that shaft power corresponds to BP power below TA and to PGS power above TA, with the exception of the period in which, during climb, the PGS is invoked at maximum rating in order to recharge the BP. Negative values of the BP power output correspond to battery charging.

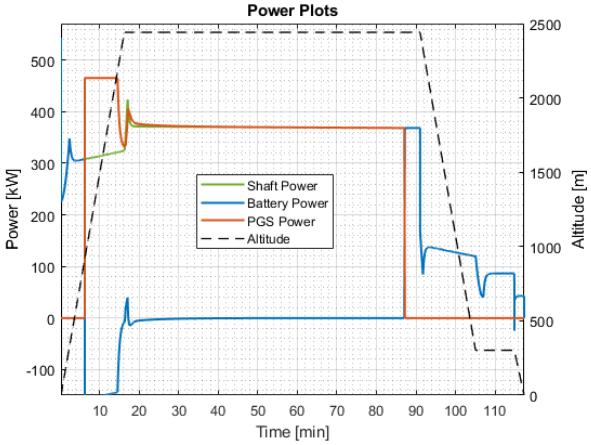

Figure 15. Time histories of shaft power (green), battery pack power (blue), PGS power (red), and altitude for the A8H.

In order to assess the A8H capabilities in off-design conditions, a payload-range trade-off study was conducted, considering the substitution of shares of payload with equal quantities of fuel. Fig. 16 shows the results obtained, related to the mission range sensitivity upon the progressive substitution of all passengers and baggage with an equal mass of fuel. This corresponds to the complete envelope of usage for the vehicle, from the design mission at full payload (8 passengers) to the ferry-range mission (no passengers on board). The slope of the curve depicting the range as a function of fuel mass has a slope of 0.32 km/kg. It is thus seen that trading-off two, four, or six passengers yields an increase in range of 92% (reaching 1,250 km), 174% (1,780 km), and 285% (2,500 km), respectively. The ferry range reaches 3,100 km. In addition to the microfeeder role, this flexibility may be conveniently exploited in more general passenger/cargo roles for point-to-point connections.

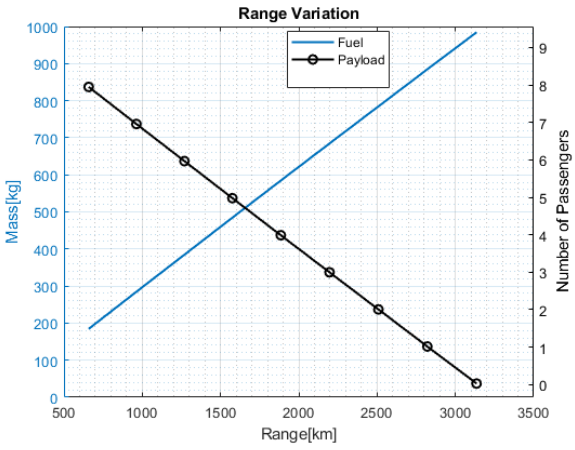

Figure 16. Payload-range diagram for the A8H.

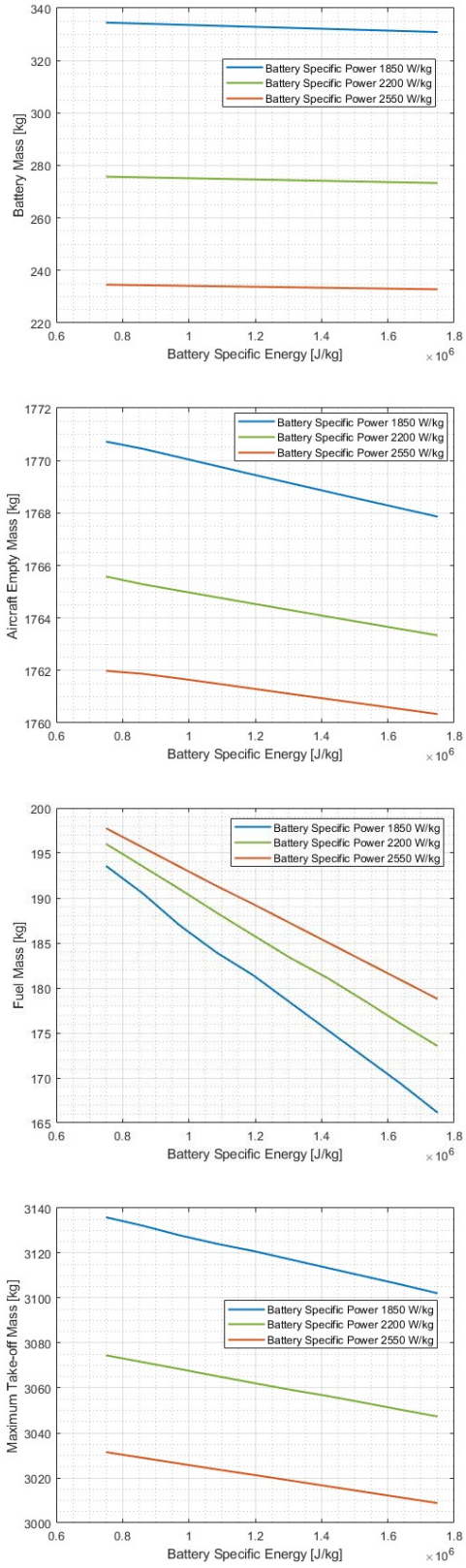

Figure 17. Sensitivity of battery pack mass (top), airframe mass (middle high), fuel mass (middle low), and maximum take-off mass (bottom) on battery energy and power densities for the A8H.

Finally, sensitivity studies of the design point for the A8H have been carried out by considering a number of design parameters. Here, the results concerned with battery technology are shown. Fig. 17 shows the trends of BPM, AM, FM, and MTOM with respect to battery specific energy and specific power, according to the same percent variations as seen for the A8E.

In the top graph, it is apparent that, while specific power greatly affects battery sizing, specific energy has a much lower effect on BPM. This is the result of the fact that the battery is always sized according to power requirements, which implies that stored energy is always exceeding that needed for the mission. Therefore, this case is generally opposite to the behaviour seen for the A8E.

It is observed that, while BPM varies by tens of kg in the considered specific energy range, the corresponding variation for the AM is limited to a few kg, while FM is also significantly sensitive. Indeed, as battery energy increases, less and less fuel is needed to perform the mission, even if the battery mass is not changed much. The MTOM changes inherit the sensitivity of BPM and FM.

6. OPTIMAL HYBRID-ELECTRIC VERSION

As the A8H has been conceived as a retrofit of the A8E, which was optimally sized, it is only natural that the former represents a sub-optimal solution for its design range mission. Therefore, it is of interest to compare the results obtained thus far with the output of a clean-sheet design procedure, carried out by running the HYPERION tool without any constraint on airframe mass and/or MTOM, in order to fulfil the A8H design range mission.

The new design solution, termed A8HO, is characterized by a different MTOM and mass breakdown, as seen in Tab. 1, third column. In particular, when compared to the A8H, the MTOM is reduced by 8.6%, the airframe mass by 13.2%, the EM mass by 7.7%, the PGS mass by 8.6%, the BP mass by 8.4%, and the fuel mass by 10.3 %. This entails, taking into account the 10% residual fuel at mission end, that the A8HO burns 17 kg of fuel less than the A8H to perform the same 655 kg-long mission.

Tab. 5 shows the values of power installed and reference wing surface for the two serial HE variants. The A8HO value for the former is reduced to 8.6% and for the latter by 10.4% with respect to the A8H (and the A8E as well).

Table 5. Sizing data for the A8 HE variants.

	A8H	**A8HO**
Shaft power [kW]	544	497
Wing surface [m^2]	20.2	18.1

In conclusion, significantly lower costs can be expected for the optimal version in relation to both production (thanks to the general reduction in

component weights) and operation (given the reduction in fuel burned and the lower BP recharging needs on ground). In addition, advantages in eco-sustainability can be seen with respect to chemical emissions (lower fuel consumption) and acoustic footprint (lower shaft power). A novel methodology for the assessment of the environmental impact of HE aircraft can be found in [16].

7. CONCLUSION

The present contribution introduces the design of a family of 8-passenger, twin-propeller commuter airplanes intended to fulfil the microfeeder role in a short-haul air transportation network. The preliminary studies clearly show that a market opportunity exists for this role and lead to the drafting of top-level aircraft requirements (TLARs). By using a novel preliminary sizing tool dedicated to electric-powered aircraft, a series of design solution were obtained.

The first, a pure-electric one, complying with all the TLARs, was chosen for a complete maturation through a preliminary design loop. Based on these results, a second solution, featuring a serial hybrid electric retrofit of the former was designed and analysed. This was found to offer significantly higher range performance compared to the first. Therefore, a novel serial hybrid-electric design has been considered, seeking an optimal solution for the design mission range of the second variant.

A discussion of the main results for the three variants was carried out, showing the resulting design specifications, their sensitivity to changes in design parameters, and the time evolution of energy- and power-related quantities along the sizing missions.

The discussion pinpoints the fact that design solutions for electric-powered aircraft need accurate sizing procedures, capable of integrating all the aspects relevant to energy, power, mass and dimensions. Simple substitutions of core elements in the sizing procedure, without guaranteeing the full coupling inherent to the preliminary sizing process, yield non-optimal solutions and may hinder the feasibility assessment of a given design solution.

8. ACKNOWLEDGEMENTS

The authors are indebted to former Politecnico di Milano students Arditi, M., D'Ascenzo, A., Montorfano, G., Poiana, G., Rossi, N., Sesso, M., and Spada, C., for the initial conception and preliminary design developments of the proposed aircraft concept.

9. FUNDING

This research was partially funded by the EU Horizon 2020 research and innovation program, under project MAHEPA, GA N. 723368.

10. REFERENCES

[1] Krein, A. & Williams. G. (2011). Flightpath 2050: Europe's vision for aeronautics. In Proc. Innovation for Sustainable Aviation in a Global Environment, 6th European Aeronautics Days, Madrid, Spain.

[2] Trainelli, L. & Perkon, I. (2019). MAHEPA – A Milestone-Setting Project in Hybrid-Electric Aircraft Technology Development. In Proc. More Electric Aircraft Conference (MEA 2019), Toulouse, France.

[3] Arditi, M., D'Ascenzo, A., Montorfano, G., Poiana, G., Rossi, N., Sesso, M., Spada, C., Riboldi, C.E.D. & Trainelli, L. (2018). An Investigation of the Micro-Feeder Aircraft Concept. In Proc. Advanced Aircraft Efficiency in a Global Air Transport System Conference (AEGATS 2018), Toulouse, France.

[4] Anonymous (2017). Air transport statistics. Eurostat - Statistics Explained.

[5] Anonymous (2016). Transport and Mobility 2016. Centraal Bureau voor de Statistiek.

[6] Bigoni, F., Moreno-Perez, A., Salucci, F., Riboldi, C. E. D., Rolando, A. & Trainelli, L. (2018). Design of Airport Infrastructures in Support of the Transition to a Hybrid-Electric Fleet. In Proc. Advanced Aircraft Efficiency in a Global Air Transport System Conference (AEGATS 2018), Toulouse, France.

[7] Riboldi, C. E. D., Bigoni, F, Salucci, F., Rolando, A. & Trainelli, L. (2019). Switching to Electric Propulsion: Aero Club Fleet and Infrastructure Sizing. In Proc. XXV Congresso Nazionale AIDAA, Roma, Italy.

[8] Salucci, F., Riboldi, C. E. D., Trainelli, L. & Rolando, A. (2020). Optimal Sizing and Operations of a Battery Recharging Infrastructure for a Regional Airport. In Proc. Aerospace Europe Conference (AEC 2020), Bordeaux, France.

[9] Bruglieri, M., Marchionni, A. M. & Trainelli, L. (2019). Optimization of the Demand Satisfied by a 'Micro-Feeder' Hybrid-Electric Air Transport Service. In Proc. XXV Congresso Nazionale AIDAA, Roma, Italy.

[10] Trainelli, L., Bruglieri, M., Salucci, F. & Gabrielli, D. (2020). Optimal Definition of a Short-Haul Air Transportation Network for Door-to-Door Mobility. In Proc. Aerospace

Europe Conference (AEC 2020), Bordeaux, France.

[11] Trainelli, L., Riboldi, C. E. D., Salucci, F. & Rolando, A. (2020). A General Preliminary Sizing Procedure for Pure-Electric and Hybrid-Electric Airplanes". In Proc. Aerospace Europe Conference (AEC 2020), Bordeaux, France.

[12] Trainelli, L., Salucci, F., Rossi, N., Riboldi, C. E. D. & Rolando, A. (2019). Preliminary Sizing and Energy Management of Serial Hybrid-Electric Airplanes. In Proc. XXV Congresso Nazionale AIDAA, Roma, Italy.

[13] Ainsworth, F. (2016). Li-S Batteries for Energy Storage Applications. OXIS Energy Ltd.

[14] Roskam, J. (2003). *Airplane Design: Parts I through VIII*. Roskam Aviation and Engineering Corporation.

[15] Airoldi, A., Bettini, P., Lanzi, l. & Sala, G. (2005). GLARE at Politecnico di Milano: Experiments and Computations. In Proc. 31st European Rotorcraft Forum (ERF 2005), Firenze, Italy.

[16] Riboldi, C. E. D., Mariani, L., Trainelli, L., Rolando, A. & Salucci, F. (2020). Assessing the Effect of Hybrid-Electric Power-Trains on Chemical and Acoustic Pollution. In Proc. Aerospace Europe Conference (AEC 2020), Bordeaux, France.